

# Fundamental Analysis of Cold Die Compaction of Reinforced Aluminum Powder

S. M. El-Katatny, A.E. Nassef, Aly El-Domiaty, W. H. El-Garaihy

**Abstract**— Aluminum Matrix Composites (AMCs) are used in many automotive and aerospace applications. The aluminum reinforced composites powder is compacted at room temperature or at elevated temperature according to the required properties of the product. In the present work, simple analytical model is used to elevate the green density as a function of the applied pressure in die compaction. Aspects die ratio as well as friction between wall and powder and powder itself are considered in the analysis. Experiments are performed on die compaction of Al-4Cu metal matrix composites. The results of the experimental finding are compared with the predicted results obtained from the simple model introduced.

**Index Terms**— Powder metallurgy, green density, theoretical density, Al-4Cu alloy.

## I. INTRODUCTION

Powder Metallurgy (PM) is defined as "the production of engineering components from metal powder without passing through the molten state" [1]. PM technique has been capable of processing a broad spectrum of materials for a wide range of applications, from automotive to power transmission tools, aerospace and house-hold applications. PM was proven to be a sound technique for producing Metal Matrix Composites (MMCs) which have been regarded as excellent engineering material candidates for meeting service properties such as high specific strength, toughness, stiffness, wear and corrosion-resistance. The MMCs consist of a monolithic pure metal or alloy as a matrix, and different type of materials like monolithic metals, ceramics or intermetallics. Reinforcement is introduced to the matrix in the form of fibers (continuous/short), whiskers, or dispersing partials. Choice of particle-reinforcement over other types (fibers or whiskers) is due to their isotropic properties and low cost [2, 3].

Generally P/M components can be produced by two techniques, firstly cold compaction following by sintering or secondly forming operation like extrusion in order to obtain bonding between particles and getting the required properties. Secondly is hot compaction which requires to heat metal

powder before compaction. Normally metal powders die compaction consists of number of stages, firstly initial compaction which involves particles rearrangement. The physical properties such as, particles size and shape are greatly influence this initial stage. This is followed by the elastic-plastic deformation, and here the mechanical properties and the quality of the particles are important factors, which control the compressibility behavior of the powder. The final stage of compaction is almost totally an upsetting of the bulk material.

There are multi models describe the plasticity behavior of PM during compaction, among these plasticity models Kuhn and Downey [4], Shima and Oyane [5], and Fleck-Gurson [6, 7]. They express the hydrostatic and deviatoric stresses in terms of the yield stress of the solid material and the yield stress of the partially dense material found in a part during compaction. The second family of plasticity models is for granular materials. These models include Drucker-Prager [8], Mohr-Coulomb, and Cam-Clay [9] among others. Granular models are suitable for all stress and strain paths, not just particular loading paths. The most used model is Drucker-Prager cap model (DPC) [10].

## II. THEORETICAL POWDER COMPACTION BACKGROUND

Most properties of a PM part are closely related to its final density. Density is expressed as relative density (RD), which is defined as the ratio of green density to theoretical density as given in Eq.1 [11],

$$RD = \frac{\rho_g}{\rho_{th}} \quad (1)$$

where  $\rho_g$  and  $\rho_{th}$  are green and theoretical density respectively. In practice, PM parts less than 75% of relative density considered to be low density; those above 90% are high density; and those in between 75% and 90% are considered as medium density [11].

By analyzing a small element of a compacting powder sample as shown in Fig. 1.a, the axial stress can be related to the compacting pressure. The analysis assumed axial symmetry and take into account the geometry of the element. Both the radial stress and the coefficients of friction were assumed to be constant [12].

**Manuscript received March 18, 2015.**

**Sally Mahmoud Elkatatny**, Mechanical engineering Department, Suez Canal University, Egypt.

**Ahmed Elsaied Nassef**, Production and Mechanical design Department, Port-Said University, Egypt.

**Aly El-Domiaty**, Mechanical engineering Department, Suez Canal University, Egypt.

**Walid Hassan El-Garaihy**, Mechanical engineering Department, Suez Canal University, Egypt.

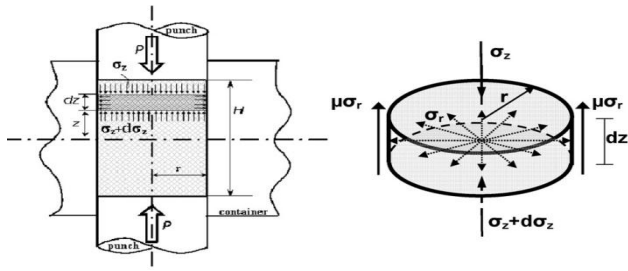


Fig.1.a

Fig.1.b

Fig. 1 Schematic diagram of compacting tools and stresses on compacted element [12].

The equilibrium of the disk element shown in Fig. 1.b gives the equilibrium equation in Z direction. Since there is no change in the diameter of the compacted powder, by using the expressions of Levy misse for plastic flow of metal, it follows that the state of stresses  $\sigma_r = \sigma_\theta$ . Using the von misse criterion for the effective stress of the bulk material ( $\bar{\sigma}$ ), Eq. 2 is obtained,

$$\frac{\sigma_z}{\bar{\sigma}} = \left[ 1 + \frac{P_a}{\bar{\sigma}} \right] \left[ \exp \left\{ \frac{\mu(H-2z)}{r_f} \right\} \right] - 1 \quad (2)$$

where  $P_a$ ,  $H$ ,  $z$ ,  $r_f$ ,  $\mu$  are the compact external punch pressure applied by the punches from both ends simultaneously, the instantaneous height of the compact cylinder, current height of the element, die radius of container and coefficient of friction between powder/wall container interface respectively. The effective stress during compaction as a function of the yield strength of the bulk material ( $\bar{\sigma}$ ) can be calculated from Eq. 3 taken into account the internal friction between particles ( $\mu_i$ ) and the geometry of the particles,

$$\bar{\sigma} = \lambda^{-1} \sigma_{yc} \left( \frac{1 + \mu_i}{1 - \mu_i} \right) \quad (3)$$

where  $\sigma_{yc}$  is the yield stress of the bulk material and  $\lambda$  is the shape factor of the particles. This ratio ( $\lambda$ ) characterizes the surface configuration of the particle, where the surface area of the particle is compared with some linear dimensions [13, 14]. The theoretical green density for a compact at any compression stage is a function of the compacting pressure, the friction between powder and die wall as well as the friction between powder particles and the die geometry can be obtained by Eq. 4. In the present analysis the radial stress and friction coefficients are assumed to be consists.

$$\rho_g = \rho_p + (\rho_t - \rho_p) \left( 1 - e^{-\frac{\sigma_z}{\bar{\sigma}}} \right) \quad (4)$$

where  $\rho_p$  is tap density.

### III. EXPERIMENTAL PROCEDURE

Aluminum powders (99.9% purity,  $\approx 25 \mu\text{m}$  mean size) were mixed by shaking with 4wt. % copper powders (99.9% purity,  $\approx 10 \mu\text{m}$  mean size). The powder was poured into a die cavity of 20 mm in diameter and 90 mm in depth made of QRO 90 Supreme. Die compaction is carried out on a Shimazu universal testing machine which has 200 ton (2 MN) capacity. The compaction method was a single action die method. The die was lubricated with graphite in order to reduce friction

between die and die wall. The upper punch was brought into contact with tapped powder in the cylinder.

This was followed by applying an axial load, which caused the powder to be compressed, and subjected to high compressive stresses. At the end of the compaction stroke, the upper punch was removed and the green compact was ejected out of the die.

The green density (mass per unit volume of an un-sintered compact) was determined by measuring sample dimensions and mass using a micrometer and digital balance respectively. Cold compaction processes were followed by measuring the height and the density for each of the compacted discs. After compaction, sintering processes were carried out by using electric furnace. The sintering was performed by heating the discs at  $580^\circ\text{C}$  for duration of 2hrs after that, the discs were left to cool to room temperature in the furnace. Ageing process at  $165^\circ\text{C}$  for 2hrs was applied as a second sintering and left the discs to cool in the air [15].

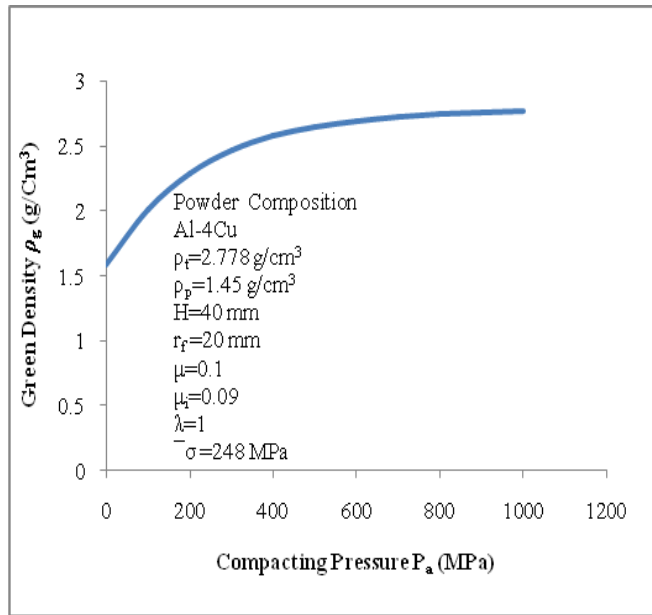
### IV. RESULTS AND DISCUSSION

Several empirical and semi-empirical expressions relating pressure and relative density during compaction of metal powder had been proposed, this is due to the complexity of the dynamic variation of the parameters during the compaction making it extremely difficult to establish relationships between the process variables.

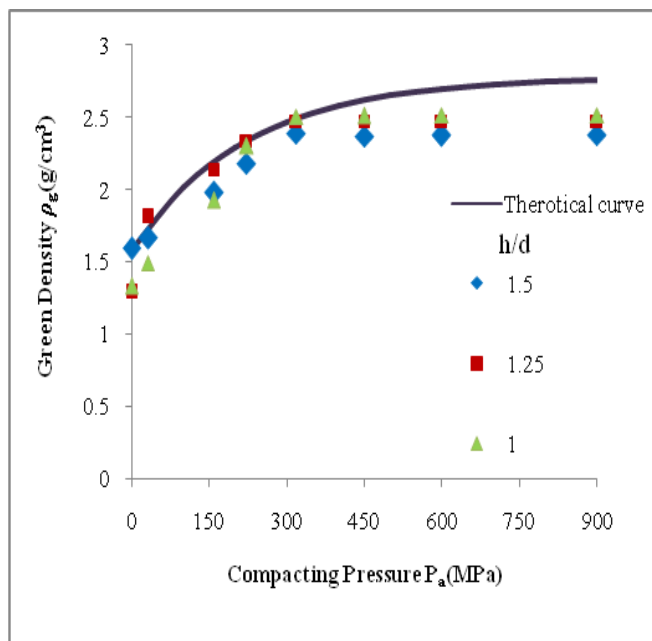
From Eq. 4, it can be revealed that the green density depends on the powder properties, geometry of the compacted sample and process variables. From the present analysis, the green density can be predicted from Eq. (4) by knowing the tap and the bulk material densities, geometry of the initial and final compacted powder and the effective compressive stress of the bulk, friction conditions, and by incrementing the applied pressure values. This finally leads to the theoretical plot of the green density at any applied pressure stage. The theoretical green density relates to compacting pressure according to Eq. (4) for Al-4Cu alloy as shown in Fig. 2a and it increases with increase the compacting pressure. Fig. 2b shows a comparison between the theoretical and experimental values of green density carried out at different height to diameter ratios ( $h/d$ ) of al-4cu alloy as a function of compacting pressure. For all compaction tests, green density increases monotonically with increasing pressure, but the slope of curves decreased, indicating a lower compressibility at higher loading in the studied pressure range. Also it can be realized that, the theoretical predictions from the model showed reasonably good agreements with experimental data at the different values of  $h/d$ .

The compaction of powders has been indicated to be a three-stage process [16]. At the initial compaction stage (0–50MPa), particle re-arranged which occurs at the very beginning of compaction and does not contribute significantly to the densification of spherical powders. At the second stage (50–225 MPa), the cold compaction behavior exhibited high densification rate detected from the steeper slope of the initial compaction curve. This may come from the fact that the inter-particle open pores of loose randomly packed aggregates were greatly reduced. During this stage, the

particles are flattened and brought closer to form additional contacts.



(a)



(b)

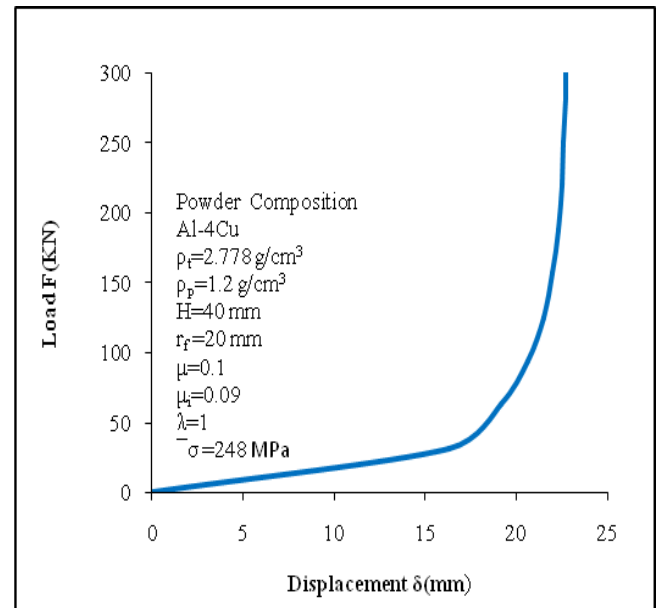
Fig. 2 (a) theoretical green density for Al-4Cu alloy, (b) Comparison between theoretical and experimental green density for Al-4Cu alloy.

The rate of increase in density values at higher loading (225–900 MPa), as revealed from the plots of Fig. 2b, was found to be apparently less, due possibly to the friction between the particles increased with the increment of applied pressure and the refinement of particle size, which hindered the compression of the powder, leading to the sluggish of densification rate.

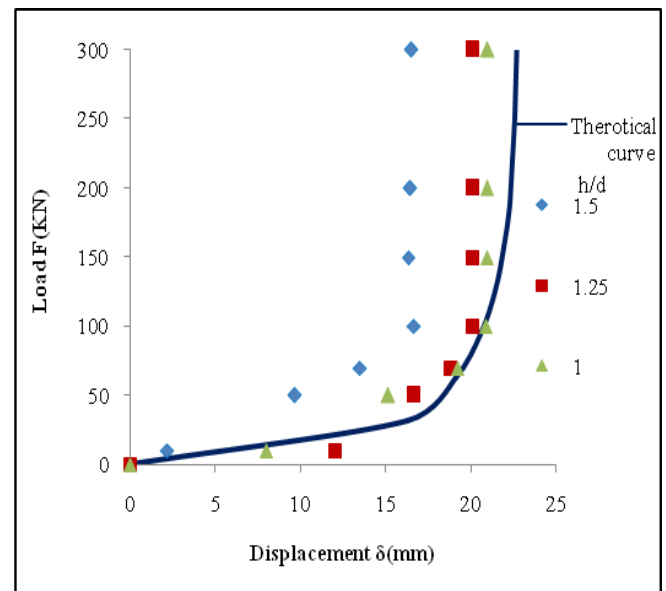
Accordingly, increasing the compacting pressure can assist all three porosity reduction mechanisms (movement of particles into voids, deformation of particles, and flattening of the

microscopic and submicroscopic features on the particle surface). As compaction pressure increases, the distance between powder particles gets closer and the destruction of the oxide layer on the surface of powders is accelerated, resulting in increased green density [17].

Cold compaction processing at pressure of 450, 600 and 900 MPa revealed an increase in the relative densities and a decrease in the porosity of Al-4Cu alloy cold compacted discs. On the other hand, decreasing the value of aspect ratio  $h/d$  from 1.5 to 1 for the alloy resulted in decreasing the percentage of porosity accompanied with increasing the relative density of the Al-4Cu discs as shown in Fig. 4.



(a)



(b)

Fig.3 (a) Theoretical for Load-Displacement diagram Al-4Cu alloy,

(b) Comparison between theoretical and experimental Load-Displacement diagram for Al-4Cu alloy

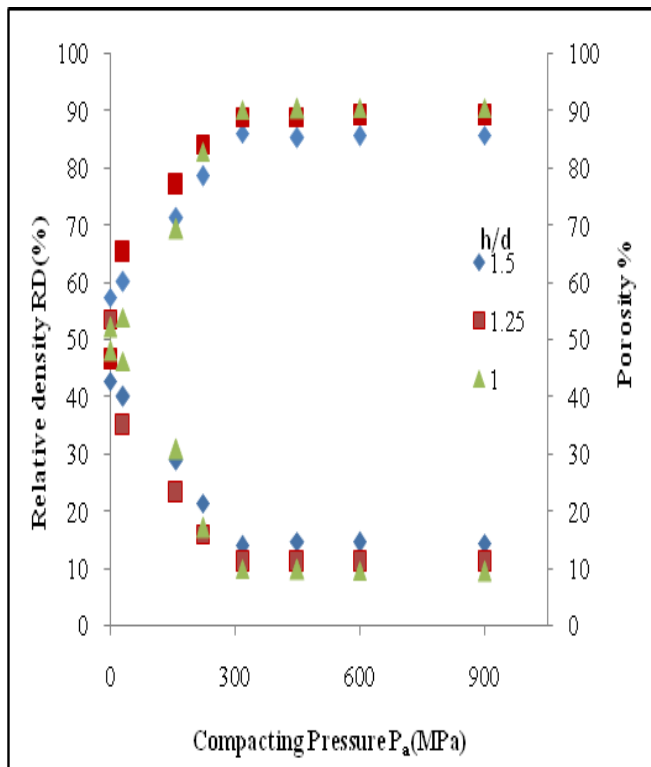


Fig.4 Relation between the relative density, the porosity and compacting pressure at different h/d ratios for Al-4Cu alloy.

Accordingly, the mechanical properties of any product via powder metallurgy technique are dependent on the porosity within the obtained product. Moreover, the density of PM product is a basic criterion for the evolution of the soundness and hence mechanical properties of the product.

Fig.5 shows the relation between the Hv-values and compacting pressure at different h/d ratios for Al-4Cu alloy. From Fig. 5, it was clear that, increasing of the compacting pressure resulted in a significant increase in the Hv-value of the cold compacted discs. Moreover, decreasing the h/d ratio from 1.5-up to-1 demonstrated an additional improvement in the Hv-value of the Al-4Cu alloy discs.

The most important data deduced from the compression test is the compressive strength, since it reflects the overall mechanical behavior of the Al-4Cu alloy discs cold compacted at different processing parameters. Moreover, the compression test provides an indication of the level of ductility as introduced by El-Domiati et al. [18].

The compressive properties of Al-4Cu alloy processed at different h/d ratios as a function of compacting pressure were presented in Fig.6. From Fig.6 it can be concluded that, increasing the compacting pressure resulted in an increase in the yield strength (YS) of the cold compacted discs. Moreover, decreasing the value of h/d resulted in increasing the yield strength (YS) of the Al-4Cu alloy discs. A similar trend was recorded for the compressive strength. Accordingly, the improvement of the hardness and the compressive strength can be attributed to the enhancement of the density due to increasing the compacting pressure or decreasing the h/d ratio.

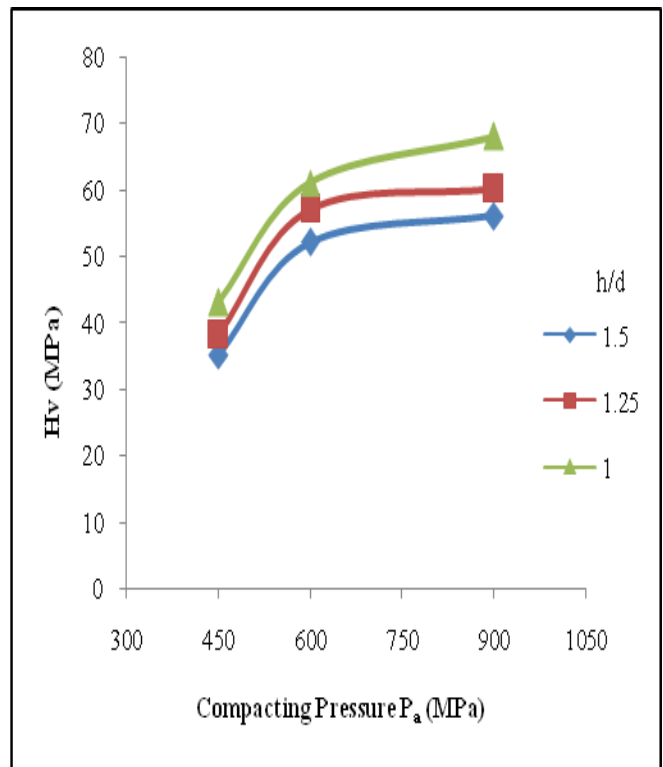


Fig. 5 Plotting of the Hv-values as a function of compacting pressure at different h/d ratios for Al-4Cu alloy.

Representative micrographs at center of Al-4Cu alloy discs compacted at different compacting pressure shown in Figs. 7. All micrographs were taken in the as-polished and etched condition at a magnification of 50x. Observation of micrographs indicated that at the lower compaction pressure, the compacts were relatively porous.

The copper particles present within the structure were significantly less deformed into aluminum matrix. It was visible that the cold compacted samples showed irregular particle shape and inhomogeneous particle size distribution after compaction, with a number of pores still remaining, which also varied considerably with different pressures.

During sintering of Al alloy, the solid state diffusion of Cu takes place into Al, and the solubility of Cu reaches up to 5.8% at temperatures above 548 °C [17]. When Cu is saturated in  $\alpha$  (Al) phase around 600 °C, Cu in the liquid phase does not solute into Al but form Cu-rich phase. This Cu-rich phase moves to inter-particle spacing or to grain boundaries so that the densification can be achieved. In the Al-4Cu alloy, Fig. 7 shows Cu-rich phases in grain boundaries which aid the densification during sintering.

As the sintering temperature reach 548 °C the Al-Cu<sub>2</sub> Al ( $\theta$ -phase) eutectic is formed at the interfaces of the neighboring aluminum and copper powder particles [19] and it facilitates the decomposition of aluminum oxide. This promotes interparticale diffusion of Al powders and enhances the mechanical properties of the sintered compacts.

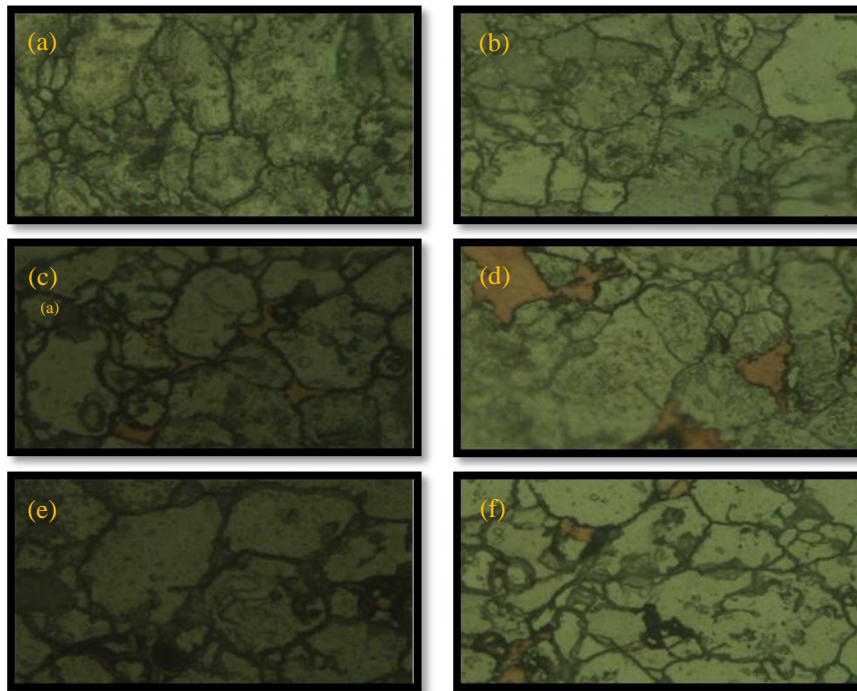


Fig. 7 OM Micrographs of Al-4Cu alloy cold compacted at (a, b) 450Mpa, (c, d) 600 MPa and (e, f) 900 MPa with different h/d of (a, c, e) h/d=1.5, (b, d, f) h/d=1, 50x.

## V. CONCLUSION

Powder compaction is influenced by multi factors. The major factor is the compacting pressure. Increasing the compacting pressure leads to increasing densification and reducing voids between particles. As the compacting pressure increases, the green density, relative density and mechanical properties such as yield strength and ultimate tensile strength increase.

## VI. REFERENCES

- [1] Li, Y. Y., Ngai, T. L., Zhang, D. T., Long, Y., Xia, W., "Effect of die wall lubrication on warm compaction powder metallurgy," *Journal of Materials Processing Technology*, 129, 354-8, 2002.
- [2] Coube, O., Riedel, H., "Numerical simulation of metal powder die compaction with special consideration of cracking," *Powder Metallurgy*, 43(2), 123-31, 2000.
- [3] Ngai, T. L., Chen, W., Xian, Z., Wen, L., Wu, Y., "Die wall lubricated warm compaction of iron-based powder metallurgy metal," *Transactions of Nonferrous Metals Society of China*, 12(6), 1095-8, 2002.
- [4] H. A. Kuhn and C. L. Downey, "Deformation characteristics and plasticity theory of sintered powder materials," *International Journal of Powder Metallurgy*, vol. 7, pp. 15-25, 1971.
- [5] S. Shima and M. Oyane, "Plasticity theory for porous metals," *International Journal of Mechanical Sciences*, vol. 18, pp. 285-91, 1976.
- [6] N. A. Fleck, L. T. Kuhn, and R. M. McMeeking, "Yielding of metal powder bonded by isolated contacts," *Journal of the Mechanics and Physics of Solids*, vol. 40, pp. 1139-1139, 1992.
- [7] A. L. Gurson, "Continuum theory of ductile rupture by void nucleation and growth. I. Yield criteria and flow rules for porous ductile media," *Transactions of the ASME. Series H, Journal of Engineering Materials and Technology*, vol. 99, pp. 2-15, 1977.
- [8] D. C. Drucker and W. Prager, "Soil mechanics and plastic analysis or limit design," *Quarterly of Applied Mathematics*, vol. 10, pp. 157-165, 1952.
- [9] K. H. Roscoe, A. N. Schofield, and A. Thurairajah, "Yielding of clays in states wetter than critical," *Geotechnique*, vol. 13, pp. 211-240, 1963.
- [10] L.H. Han, J.A. Elliott, A.C. Bentham, A. Mills, G.E. Amidon, B.C. Hancock, "A modified Drucker-Prager Cap model for die compaction simulation of pharmaceutical powders," *International Journal of Solids and Structures*, vol. 45, pp.3088-3106,2008.
- [11] [www.mpif.org/designcenter/dense\\_props.asp?linkid=49](http://www.mpif.org/designcenter/dense_props.asp?linkid=49)
- [12] H.A. Al-Qureshi, M.R.F. Soares, D. Hotza, M.C. Alves, A.N. Klein, "Analyses of the fundamental parameters of cold die compaction of powder metallurgy," *Journal of materials processing technology*, vol. 199, pp. 417-424, 2008.
- [13] MPMF Standard 35, "Materials Standards For P/M Structural Parts," Metal Powder Industries Federation, Princeton, USA, 1994.
- [14] Hausner, H.H., Mal, M.K., *Handbook of Powder Metallurgy*. Chemical Publishing Co., New York, 1982.
- [15] Zamri Yusoff, Shamsul Baharin Jamaludin, "The Influence of Particle Sizes and Compaction Pressure on Surface Hardness of Aluminum Composite Fabricated Via Powder Metallurgy," *Australian Journal of Basic and Applied Sciences*, 5(11): 133-140, 2011.
- [16] H.F. Fischmeister, E. Arzt, "Densification of powders by particle deformation," *Powder Metall.* 26 (1983) 82-88.
- [17] Min Chul OH, ByungminAhn, "Effect of Mg composition on sintering behaviors and mechanical properties of Al-Cu-Mg alloy", *Trans. Nonferrous Met. Soc. China* 24(2014) s53-s58.
- [18] Aly El-Domiaty and M. Shaker, "A Note on the Workability of porous-steel performs," *J. of Materials Processing Technology*, 1990.
- [19] A. E. Nassef, G.A. Ebrahim and A.A. El-Baghdady, "Mechanical and Microstructure Characteristics of Al-4Cu/Al<sub>2</sub>O<sub>3</sub> MMCs Produced Via PM Techniques", *J. of engineering and applied science, faculty of Eng., Cairo Uni.* vol. 50, No.2, PP 371-386, 2003.